One-step deposition of ultrafiltration SiC membranes on macroporous SiC supports

UNIVERSITÀ DEGLI STUDI DI TORINO

One-step deposition of ultrafiltration SiC membranes on macroporous SiC supports

Katja König[a], Vittorio Boffa,[a*] Bjarke Buchbjerg,[a] Ali Farsi[a], Morten L. Christensen[a], Giuliana Magnacca[b], Yuanzheng Yue[a]

[a]Section of Chemistry, Aalborg University, Sohngårdsholmsvej 57, DK9000 Aalborg, Denmark.

[b]Universitá di Torino, Dipartimento di Chimica and NIS Centre, Via P.Giuria 7, 10125 Torino, Italy.

* Corresponding author. Tel.: +45 9940 3579.

E-mail address: vb@bio.aau.dk (V. Boffa)

Abstract

We fabricated new, defect-free SiC membrane for potential ultrafiltration applications by conducting pyrolysis of allylhydrido polycarbosilane in the presence of submicron α-SiC particles. The SiC membrane was developed on a commercial macroporous SiC support by a low-temperature-process in which allylhydrido polycarbosilane acted to bond together crystalline α-SiC particles to form a porous layer. The suspensions of α-SiC powder and allylhydrido polycarbosilane in hexane or hexane/tetradecane were used for membrane fabrication by dip-coating. By using optimized hexane suspension with 5% w/w α-SiC powder and mass ratios of allylhydrido polycarbosilane to SiC powder of 0.6 and 0.8, we obtained defect-free and uniform mesoporous membranes in a single coating procedure. No defects were found on the surface of these membranes by scanning electron microscopy. Moreover, during filtration tests, these membranes showed a water permeability of 0.05-0.06 L $(m^2$ h bar$)^{-1}$ and retention higher than 93% for polyethylene glycol (PEG) with a molecular mass of 100 kDa. Retention for PEG with molecular masses of 1 kDa, 8 kDa and 35 kDa was between 25% and 71%.

Keywords: SiC membranes, ultrafiltration, polycarbosilane

1 Introduction

Nowadays, ceramic membranes are applied to a large number of ultrafiltration processes, including water purification, food and beverage processing, bioreactors, and molecular separation systems in the petrochemical and chemical industry [1–3]. Compared with polymeric membranes, ceramic membranes have higher thermal, mechanical, and chemical resistances. In particular, mesoporous γ-alumina has been frequently considered as a material for ultrafiltration membranes because defect-free films of this material can be easily deposited on macroporous supports by the sol-gel method. However, γ-alumina membranes do not demonstrate high enough chemical stability in either strongly acidic or basic environments [4]. In comparison to γ-alumina, silicon carbide (SiC) has a better chemical stability in harsh conditions, for example in corrosive and high-temperature environments [5,6]. For this reason, SiC is a convenient membrane material to withstand repeated aggressive cleaning, steam sterilization and autoclaving. As a result, SiC is well suited to food and biopharmaceutical processing [7,8]. Moreover, compared with other polymeric and oxide materials such as titania and zirconia, SiC membranes are exceptionally hydrophilic and exhibit low fouling [9,10].

However, due to the covalent nature of the Si-C bonds, high sintering temperatures and the addition of sintering aids are usually required for the production of SiC ceramics [11]. This requirement has two primary implications: (i) SiC membrane processing is costly and (ii) it is difficult to fabricate thin SiC layers in the microporous and mesoporous range by partial sintering [13]. Furthermore, the use of SiC membranes is rather limited today and it is mostly relegated to microfiltration processes. Nevertheless, alternative processing routes for the preparation of mesoporous SiC at reduced temperatures, based on the conversion of metaloorganic polymers to SiC, are now available [14,15]. The fabrication of polycarbosilane (PCS)-derived SiC membranes has been addressed concerning gas-separation applications [15–18]. Since the conversion of polymer precursors to SiC incurs a 20–

30% volume film shrinkage, it is necessary to repeat the deposition and the consecutive pyrolysis steps several times in order to obtain defect-free films [12]. Moreover, direct coating of PCS cannot be performed without avoiding consistent penetration of the polymeric precursor in the pores of the macroporous support, which typically have size ≥ 100 nm [19]. On the contrary, combination of pre-formed SiC particles and PCS makes it possible to achieve thicker SiC coatings without cracks by a single deposition step [12]. Up until now, this approach has been used for the deposition of thick intermediate layers for gas separation membranes [17]. However, to the best of our knowledge, the fabrication of PCS-derived mesoporous SiC membranes on SiC macroporous supports for ultrafiltration applications has not been realized yet. Furthermore, only a few studies have actually emphasized the important role of the composition of the coating suspension in fabrication of defect-free mesoporous PCS-derived coatings [14, 15].

In this context, we focus on the development of PCS-derived SiC mesoporous membranes supported on commercial macroporous SiC carriers for use in ultrafiltration. α-SiC particles were used to effectively cover the pores of the support, while PCS served to connect the particles and to ensure good membrane adhesion to the surface of the support. The application of a mesoporous ultrafiltration membrane on a macroporous support is not trivial, because pore size, thickness, and defect density of the coated film depend on the composition of the coating suspension, on the fabrication conditions, and also on the roughness and the surface inhomogeneity of the supports [20,22]. Therefore, in order to develop PCS-derived SiC mesoporous membranes, we consider several fabrication parameters. First, the coating mixture was optimized in order to obtain defect-free films. Second, two suspensions with composition in the range suitable for film deposition, were used for the membrane fabrication. The membrane morphology was investigated by transmission electronic microscopy and nitrogen adsorption porosimetry. Supported membranes were tested by measuring their water permeability and their retention for a series of poly(ethylene glycol)

molecules with different molecular masses. This technique was selected because it allows for the forecasting of the separation performances of the new membranes and comparisons with bare supports [23,24].

2 Experimental

2.1 Membrane fabrication

Commercially available α-SiC powder with an average particle size d_{50} = 0.4 μm (NF25, ESK, Germany) and allylhydridopolycarbosilane (SMP-10, Starfire, USA, herafter termed AHPCS) were used for the fabrication of nanoporous SiC thin films. Suspensions of AHPCS with the α-SiC powder were prepared in 100 mL glass bottles using *n*-hexane (Sigma Aldrich, Broendby, Denmark) or a mixture of 70% *n*-hexane and 30% *n*-tetradecane (Sigma Aldrich) as solvents. The concentration of α-SiC powder in the solvent varied from 3–7% w/w and the mass ratio of AHPCS and α-SiC powder (hereafter termed as AHPCS/α-SiC ratio) varied from 0.2–2. After treatment in an ultrasonic bath for 2 h, the suspensions were used for coating the macroporous flat SiC discs (diameter 2.5 cm, thickness 0.5 cm) supplied by Liqtech International A/S (Ballerup, Denmark).

The supports were examined for defects by scanning electron microscope (SEM, Evo60, Carl Zeiss, Oberkochen, Germany) prior to coating. The criterion for the selection of the supports for subsequent coating was no defects (particles, cracks, pinholes) larger than 100 μm on the surface. The supports were first cleaned in acetone and then heat-treated at 450 °C for 2 h in air. Polymer-derived SiC membranes were obtained by using a simple homemade apparatus for dipping in and withdrawing disks from the coating suspension at a constant rate. The disks were dipped and withdrawn at an angular speed of 1.3 rad/s. After coating, the samples were heat-treated in argon in a tube furnace (RHTH 120 600/18, Nabertherm, Lilienthal, Germany) at 200 °C for 1 h, 400 °C for 1 h, and then 750 °C for 2 h. The heating and cooling rates were 2 °C/min and 3 °C/min,

respectively. As reported by other authors, such a low heating rate makes it possible to obtain good cross-linking of amorphous SiC materials and minimizes defect formation [17,22]. In all cases a single coating was applied to the supports.

2.2 Membrane characterization

The presence of defects on the membrane surfaces and the membrane thickness values were investigated by analyzing the membrane surface and cross sections by SEM. The membrane structure and porosity were investigated on unsupported samples, which were prepared by the same heat-treatment procedure as the supported membranes. Transmission electron microscopy (TEM) images were obtained with a JEOL 3010-UHR instrument (acceleration potential: 300 kV). Samples for TEM investigation were prepared on a holey-carbon-coated copper grid by dry deposition. Specific surface area (according to Brunauer-Emmett-Teller theory, BET) and porosity were determined on about 0.2 g of unsupported sample by N_2 adsorption at the liquid-nitrogen boiling point in a gas-volumetric apparatus (ASAP2020, Micromeritics). In order to avoid undesired interferences from gaseous products from the membrane samples during the gas-volumetric determinations, the samples were outgassed in vacuum (residual pressure 10^{-5} bar) at 373 K for 8 h prior to analysis. Pore volume and pore size distribution were calculated by using the Barret-Joyner-Halenda (BJH) method [**Errore. L'origine riferimento non è stata trovata.**] applied to the entire adsorption branch of the isotherm.

2.3 Filtration tests

Filtration tests were performed on a dead-end stainless steel filtration apparatus at a static pressure of 10 bar. The filtration apparatus was designed for housing the flat SiC disks. The permeate flux

was measured gravimetrically. Different feed solutions were filtered: pure deionized water (18.2 MΩ cm), an aqueous solution of polyethylene glycol (PEG, Sigma Aldrich) of three different molecular masses (M_n), namely 1 kDa, 8 kDa, and 35 kDa, and a solution of PEG (Sigma Aldrich) of molecular mass 100 kDa. The concentration was 1 g/L for all the PEGs. The determination of the PEG concentration in the membrane feed and permeate was performed as described in details elsewhere [21] by using a size exclusion chromatography (SEC) column PolySep GFC-P interfaced with an evaporative light scattering detector. This SEC column allowed us to obtain a good peak separation for PEG masses of 1 kDa, 8 kDa, and 35 kDa, but not for 100 kDa. For this reason, the latter compound was filtered separately from the others.

3 Results and discussion

3.1 Membrane supports and coating materials

Considerable evidence suggests that the surface properties of the support (roughness, wettability, inhomogeneity, and defect density) influence the uniformity and the integrity of the coated membrane [22, 26]. Recent works [21, 29] and our preliminary tests revealed that inherent defects of commercial macroporous SiC supports challenge the development of a defect-free top layer. For this reason, high priority was given to the selection of suitable disk substrates (Fig. 1a) for membrane coatings in order to mitigate the influence of surface irregularities on the quality of the final ultrafiltration membrane. Figure 1b shows a representative SEM micrograph of surface structure of macroporous SiC disk supports used in this study. The disks have an asymmetric structure consisting of several layers with a gradual decrease in particle size from the bulk support to the top layer (Fig.1c), which has a grain size of about 300 nanometers and pore sizes up to several hundreds of nanometers. The disks have a regular surface, a water permeability > 10^3 L (m^2 bar h)$^{-1}$, and they appear to be a promising carrier for ultrafiltration membranes. Nevertheless, as

indicated by the arrows in Fig.1b, a few inhomogeneous domains are visible on the support surface, e.g., aggregates and larger grains on the surface and some larger pores.

Commercial α-SiC powder was used as a component of the suspensions for membrane coating. As shown in Fig. 2, the powder consists of particles with a narrow size distribution and an average size of 370 nm. This powder was selected because it has particles small enough to allow the formation of thin films with small interparticle pores, but also large enough to avoid penetrating the support. AHPCS was used as the polymeric precursor because it is in a liquid form, is moderately stable in air, and can yield near-stoichiometric SiC [30]. Furthermore, it has to be noted that silicon carbide is a material which is indeed hydrophilic, but it can also be easily wetted by hydrocarbons enabling fabrication of a continuous coating on the substrate [31]. Suspensions of the α-SiC powder in a solution of AHPCS and alkane were used for the fabrication of mesoporous membranes, as described in Section 2. Table 1 lists the membranes discussed in this work. The coating suspension is characterized here by three parameters: (1) the type of solvent, (2) the loading of α-SiC particles, and (3) the AHPCS/α-SiC mass ratio. These three parameters allow for the univocal definition of the coating suspensions and have been found to be key parameters to explain the defectiveness and porosity of the consolidated layers. For convenience, the type of membranes will be hereafter referred to with the designations given in Table 1.

3.2 Coating optimization

3.2.1 α-SiC powder concentration

We investigated the influence of the α-SiC powder concentration of the coating suspension on the coating quality. Suspensions with different amounts of α-SiC powder and a constant AHPCS/α-SiC ratio of 0.2 were prepared, as reported in Table 1. Fig. 3 shows the microstructures of heat-treated membranes prepared from *n*-hexane suspensions with an AHPCS/α-SiC weight ratio of 0.2

with 3% w/w (M1), 5% w/w (M2), and 7% w/w (M3) of α-SiC powder. One can see that the suspension with the lowest amount of SiC powder (M1) yielded a coating without cracks, but with insufficient coverage (Fig. 3a), whereas the suspension with the highest concentration of SiC powder (M3) yielded a coating with many cracks (Fig. 3c). On the other hand, the coating made from the suspension with 5% w/w SiC (M2) was smooth and uniform (Fig. 3b). It is well known that the powder content in the coating suspension is an important factor controlling the thickness of the coatings and consequently the formation of cracks. Crack formation is energetically favorable when the thickness exceeds a critical value [32]. Increasing the content of SiC powder and AHPCS yields more solid material in the coating. Moreover, the viscosity of the suspension increases, thus increasing the thickness of the deposited layer for constant coating conditions [333].

3.2.2 Solvent

The selection of dispersion medium can influence the film formation by changing the viscosity of the coating suspension and thus the thickness of the derived film. Furthermore, the selection of the dispersion medium can influence the drying rate of the deposited film and thus the porosity and the integrity of the consolidated film. For this reason, in this study two dispersion media were used, namely *n*-hexane and a mixture of *n*-hexane/*n*-tetradecane (30:70% V:V). *n*-hexane (C_6) has a boiling point of 68.7 °C and a viscosity of 0.295 mPas at 25 °C, and *n*-tetradecane (C_{14}) has a boiling point of 252-254 °C and a viscosity of 2.078 mPas at 25 °C [344].

Hence, the coatings prepared using a hexane/tetradecane mixture (M4–M6) were compared to those prepared from suspensions in hexane (M1–M3). Coatings M5 and M6, prepared at a α-SiC concentration ≥ 5%, exhibited extensive cracking similar to that observed in Fig. 3c for the M3 coating prepared from hexane suspensions. This observation can be explained by the fact that n-tetradecane is more viscous than n-hexane. Thus, suspensions dispersed in a n-hexane/n-tetradecane mixture are expected to yield thicker membranes than suspensions with the same solid and polymer

content but dispersed in pure hexane. For the same reason, the M4 coating shown in Fig. 4 appears to be more uniform than the M1 coating. On the other hand, the surface of the M4 coating is smooth, but contains a few hundred nanometers large pores, which were not present in the M1 and M2 coatings (Fig. 3a and b). The formation of such pores is most likely connected with the high boiling temperature of n-tetradecane. n-Tetradecane domains are expected to be still present in the coating when cross-linking of AHPCS starts at a temperature around 170 °C [355]. The evaporation of the remaining solvent at higher temperature will result in the formation of these macropores.

3.2.3 AHPCS/α-SiC ratio

The presence of macropores in the coated layer was greatly reduced when the AHPCS/α-SiC ratio was increased to 0.7–1.0, as shown in Fig. 5a and b for the M7 and M8 membranes, respectively. These two coatings indeed appear to be denser, more homogenous, and characterized by smaller pore sizes than the M4 membrane. However, when the AHPCS/α-SiC ratio was 1.7 (coating M9; Fig. 5c), many fractures were observed. Fig.5d, e and f shows the cross section SEM images of M7, M8 and M9, respectively. It can be observed that an increase in AHPCS concentration also influences the thickness of the coatings, but to a lesser extent than an increase in α-SiC powder concentration. Indeed, the measured thickness of the membrane top layer are 10 ± 9 μm for M7, 18 ± 2 μm for M8, and 19 ± 3 μm for M9. M8 and M9 have a membrane layer thickness between that measured for the nearly defect-free layer of M2 and the cracked layer of M3 membrane. Therefore, the formation of cracks in M9 membrane could be attributedto the deposition of a too thick layer. However, the cracked M9 membrane has a thickness similar to M8 membrane, for which defects were not observed. AHPCS decomposition is accompanied by significant shrinkage, which could also be the cause of the formation of large fractures in the pyrolyzed film. Hence, a suspension with an optimal AHPCS/α-Sic ratio needs to be formulated to obtain nearly

defect-free coatings with fine pores. If there is not enough AHPCS, the coating will not be continuously filled. On the other hand, if α-SiC particles are separated by a large amount of AHPCS, as in membrane M9, the shrinkage during thermal treatment can easily lead to crack formation.

3.3 Optimized membrane structure

The results of the coating optimization tests have the following implications: (i) in general, the presence of n-tetradecane in the dispersion medium yields thick layers and macropores, yielding a membrane that is not suitable for ultrafiltration application; (ii) AHPCS/α-SiC ratios higher than 0.2 but lower than 1.7 allowed for the fabrication of crack-free continuous films; (iii) when pure n-hexane was used as dispersion medium, the best layer was obtained at a α-SiC loading of 5% (M2). A graphical summary of the quality of the coated films is given in Fig. 6. Nearly defect-free films could be obtained only from suspensions within a narrow range of composition. Following these results, two optimized membranes were synthetized, namely M10 and M11. These membranes were prepared from coating suspensions similar to the one used for M2, but with a higher AHPCS/α-SiC ratio. Since the two films have similar features, only M10 is shown in Fig. . In comparison to M2 (Fig. 3b), the surface of the new coatings was more compact and uniform (Fig.7a). Fig. 7b shows the cross sections of the membrane prepared from the optimal suspension. Asymmetric structure of the SiC carrier and the top SiC membrane layer can be seen. The thickness of the final layer was estimated to be around 15 ± 2 μm.

Fig. 8 shows the TEM images of the unsupported M10 membrane. As expected, the membrane (Fig. 8a) consists of dense and crystalline polyhedral α-SiC particles bound together by the amorphous porous phase, which was formed by the decomposition of AHPCS by pyrolysis at 750 °C in Ar. In the upper left-hand side of Fig. 8b, one can clearly see that a few nanometers large

pores in the binding phase are present. This phase is expected to be amorphous since nanocrystalline β-SiC has been reported to form above 1250 ºC [366,377].

The porosimetry results for the two unsupported M10 and M11 membranes are depicted in Fig.9a and b, respectively, and the corresponding nitrogen sorption isotherms are shown in the two insets. The sorption curve of the unsupported M10 sample (5% α-SiC powder in n-hexane, AHPCS/ α-SiC=0.6) has a shape similar to a type I isotherm according to the classification proposed by the International Union of Pure and Applied Chemistry (IUPAC), i.e., associated with micropore sizes (< 2 nm) or small mesopores. Nevertheless, a narrow hysteresis loop can be observed in the range of relative pressure (p/p^0) 0.45–0.80, indicating also the presence of a small amount of large mesopores (width > 10 nm) in this sample. The curve corresponding to M11 (5% α-SiC powder in n-hexane, AHPCS/ α-SiC=0.8) could be attributed to type IV isotherm, characteristic of capillary condensation in mesopore materials. Considering the height of the isotherm knee at $p/p^0 < 0.1$, it is possible to also find micropores in the M11 sample. The adsorption isotherms were used to calculate the pore size distribution of the two membranes by applying the DFT method [26]. This method was selected because it allows determining the pore size distribution in both the mesoporous and the microporous region. As shown in Fig.9, M10 and M11 have at least two types of pores: micropores and mesopores with size smaller than 5 nm, and larger mesopores with size up to 40-50 nm. Nevertheless, consistently with the sorption isotherms, M10 shows a negligible amount of large mesopores, while in the case of M11 the volume occupied by such large pores is comparable to the one occupied by the pores smaller than 5 nm. The difference in the pore size of the M10 and M11 samples could be attributed to the fact that the suspension composition for M11 contains more AHPCS than M10. After heat treatment AHPCS shrinks by 20-30% v/v [12], thereafter larger pores are left in between the SiC particles in the M11 sample compared with the M10 sample.

Nitrogen sorption measurements also allowed determining BET specific surface area and specific pore volume for the two materials. M10 and M11 mainly consist of dense α-SiC crystallites. Thus, it is not surprising that both powders have rather low BET specific surface area (146 m^2 g^{-1} for M10 and 106 m^2 g^{-1} for M11) and specific pore volume (0.071 cm^3 g^{-1} for M10 and 0.044 cm^3 g^{-1} for M11).

3.4 Filtration tests

Filtration tests were performed on a dead-end apparatus by filtering deionized water and an aqueous mixture of polyethyleneglycol (PEG) molecules with various molecular masses. Fig. 10a shows the permeability of deionized water for the support in condition received by the supplier and for the M10 and M11 membranes. The starting supports showed a water permeability of 1800 L (h m^2 bar)$^{-1}$, which corresponds to the specifications provided by the supplier. After membrane deposition, the water permeability dropped by about 5 orders of magnitude and values of 0.05 and 0.06 L (h m^2 bar)$^{-1}$ were measured for M10 and M11, respectively. This finding is an indication that even after only one coating, the support was completely covered and no large defects were present in the active layer of the two membranes. Nevertheless, M11 shows water permeability values from 6 to 90 times lower than γ-alumina [28, 38, 39], TiO2 [40, 41], TiO2-ZrO2 [40], and SiO2-ZrO2 [42,43] membranes coated on α-Al2O3 flat and tubular supports. These ceramic oxide nano/ultrafiltration membranes have typically thickness of 1-2 μm and consist of materials with porosity between 20% and 50%. Thus, further optimization should be focused on the design of continuous mesoporous SiC layers of reduced thickness and increased pore volume. At the same time, the penetration of the coating suspension should also be prevented. However, it should be stressed that the deposition of 1-2 mm thick defect-free ultrafiltration layer on commercial

macroporous SiC supports at the present appears to be unrealistic, due to their surface coarseness and heterogeneity.

Fig. b shows the corresponding retention as a function of the PEG molecular mass for the bare support and the two membranes. As expected, the commercial SiC support has too large pores to retain a significant amount of the dissolved PEG polymers, which have average molecular masses (M_n) of 1 kDa, 8 kDa, 35 kDa, and 100 kDa and theoretical hydrodynamic diameters of 1.5 nm, 4.2 nm, 8.5 nm, and 12.5 nm, respectively [24]. A sharp increase in membrane PEG retention was observed after the coating of the mesoporous SiC layers. The retention toward the PEG with a molecular mass 100 kD was 97% for M10 and 93% for M11. Membrane retention progressively decreases by reducing the molecular mass of the permeating molecules. M10 shows a retention of 71% toward the PEG with a molecular mass 35 kDa, whereas it exhibits retention values of 45% and 25% toward the PEG with molecular masses of 8 kDa and 1 kDa, respectively. The M11 membrane shows retention values of 51% for the PEG with a mass of 35 kDa, 37% for the PEG with a mass of 8 kDa, and 32% for the PEG with a mass of 1 kDa.

Reproducibility of the membrane properties was investigated by filtration tests performed on several coated supports. When large inhomegeneities were present on the surface of the support, water permeability values were up to 4 L $(m^2\ h\ bar)^{-1}$ and PEG retention values similar to the support were observed. In the case of defect-free membranes, the PEG retention values had a standard deviation ≤ 7% for membranes prepared from the same suspension and ≤ 13% when the membranes were prepared from suspensions with the same composition but from different batches. As expected, the retention of the membranes increases with the molecular mass of the probe molecules. Nevertheless, the retention values higher than 93% for the PEG with molecular mass 100kDa do not seem to be consistent with the pore size distributions depicted in Fig.9, having the two membrane materials, especially M11, a fraction of pores with sizes above 20nm and thus

permeable to this probe. However, it should be considered that: (i) the consolidated membrane layer might have a structure slightly different from the unsupported membrane material [44], because it is formed on a rigid support and because of the penetration of part of the polymer precursor in the support pores; (ii) nitrogen sorption measurements reveal all the open pores of the membrane material, while during filtration experiment only the through membrane pores are investigated [45]. On the other hand, the results of the filtration of PEG with molecular mass < 35kDa support the difference in the pore size between the M10 and M11. Compared with M10, M11 has a larger fraction of pores larger than 5 nm and thus shows a lower retention toward PEG with molecular masses of 8kDa and 35kDa. The volume of pores small enough to retain PEG with molecular mass of 8kDa but permeable to PEG with molecular mass of 1kDa is larger for M10 than for M11; thus the difference in the retention between PEG with these two molecular masses is larger for M10 than for M11.

4 Conclusions

This work shows that it is possible to fabricate SiC ultrafiltration membranes by a simple single-step deposition method. By using 5% SiC powder and an AHPCS/α-SiC ratio equal to 0.6 and 0.8 in hexane, we can obtain defect-free mesoporous membranes after pyrolysis at 750 °C. These membranes exhibit a complex pore structure, consisting of two size orders of pores: pores smaller than 5 nm and large mesopores. The latter type of pores is especially present in the membrane material prepared at AHPCS/α-SiC ratio of 0.8. However, filtration tests suggest that both membranes have a molecular weight cut-off between 35 and 100 kD. This finding is a noticeable improvement compared with the almost-negligible PEG retention exhibited by the bare support. Water permeance of the new membranes is rather low compared with commercial γ-alumina ultrafiltration membranes. Nevertheless, the membranes studied here are already promising

considering the high stability of SiC and the simple one-step procedure here presented. Further improvements of the perm-selective properties of this type of SiC membranes are expected by further adjusting the coating composition with different fillers and by optimizing firing conditions.

Acknowledgement

This work is financially supported by the Danish National Advanced Technology Foundation (Højteknologifonden) under the project 0-59-11-1.

References

1. T. Tsuru, M. Miyawaki, H. Kondo, T. Yoshioka, M. Asaeda, Inorganic porous membranes for nanofiltration of nonaqueous solutions, Sep. Purif. Technol. 32 (2003) 105-109.
2. W.R. Baker, Membrane technology and applications, Wiley, Menlo Park, CA, 2004.
3. H. Qi, G.Z. Zhu, L. Li, N.P. Xu, Fabrication of a sol–gel derived microporous zirconia membrane for nanofiltration, J. Sol-Gel. Sci. Technol. 62 (2012) 208–216.
4. T. Van Gestel, H. Kruidhof, D.H.A. Blank, H.J.M. Bouwmeester, ZrO_2 and TiO_2 membranes for nanofiltration and pervaporation Part 1. Preparation and characterization of a corrosion-resistant ZrO2 nanofiltration membrane with a MWCO< 300, J. Membr. Sci. 284 (2006) 128–136.
5. Y. Zhou, M.B. Fukushima, H. Miyazaki, Y. Yoshizawa, K. Hirao,Y. Iwamoto, K. Sato, Preparation and characterization of tubular porous silicon carbide membrane supports, J. Membr. Sci. 369 (2011) 112–118.
6. R.J. Ciora, B. Fayyaz, P.K.T. Liu, V. Suwanmethanond, R. Mallada, M. Sahimi, T. Tsotsis, Preparation and reactive applications of nanoporous silicon carbide membranes, Chem. Eng. Sci. 59 (2004) 4957–4965.

7. S. Somiya, Y. Intomata (Eds.), 1991. SiC Ceramics-2. Elsevier, New York, NY.
8. R. Singh, E.J. Hoffman, S. Judd, Membranes Technology ebook Collection: Ultimate CD, Elsevier, Colorado Springs, USA, 2006.
9. X.H. Wang, Y. Hirata, Colloidal processing and mechanical properties of SiC with Al_2O_3 and Y_2O_3, J. Ceram. Soc. JPN 112 (2004) 22–28.
10. B. Hofs, J. Ogier, D. Vries, E.F. Beerendonk, E.R. Cornelissen, Comparison of ceramic and polymeric membrane permeability and fouling using surface water, Sep. Purif. Technol. 79 (2011) 365-374.
11. R. Riedel, G. Passing, H. Schönfelder, R. J. Brook, Synthesis of dense silicon-based ceramics at low temperatures, Nature 355 (1992) 714-717.
12. P. Colombo, G. Mera, R. Riedel, G. D. Sorarù, Polymer-Derived Ceramics: 40 Years of Research and Innovation, J. Am. Ceram. Soc. 93 (2010) 1805–1837.
13. J.-H. Eom, Y.-W. Kim, S. Raju, Processing and properties of macroporous silicon carbide ceramics: A review, J. Asian Ceram. Soc. 1 (2013) 220–242.
14. S. Zhu, S. Q. Ding, H. Xi, R. Wang, Low-temperature fabrication of porous SiC ceramics by preceramic polymer reaction bonding, Mater. Lett. 59 (2005) 595–597.
15. M. Fukushima, Y.Zhou, Y.I. Yoshizawa, H. Y. Miyazaki, K.Y. Hirao, Preparation of mesoporous silicon carbide from nano-sized SiC particle and polycarbosilane, J. Ceram. Soc. JPN, 114 (2006) 571-574.
16. M. H. Suh, W. T. Kwon, E. B. Kim, S. R. Kim, S. Y. Bae, D. J. Choi, Y. Kim, H_2 permeable nanoporous SiC membrane for an IGCC application, J. Ceram. Process. Res. 10 (2009) 359–363.
17. B. Elyassi, M. Sahimi, T. Tsotsis, Silicon carbide membranes for gas separation applications, J. Membr. Sci. 288 (2007) 290–297.

18. B. Elyassi, M. Sahimi, T.T. Tsotsis, A novel sacrificial interlayer-based method for the preparation of silicon carbide membranes, J. Membr. Sci. 316 (2008) 73–79.
19. B. Elyassi, W. X. Deng, M. Sahimi, T. T. Tsotsis, On the use of porous and nonporous fillers in the fabrication of silicon carbide membranes, Ind. Eng. Chem. Res. (2013) 52 10269–10275.
20. P. M. Biesheuvel, H. Verweij, Design of ceramic membrane supports: permeability, tensile strength and stress, J. Membrane Sci. 156 (1999) 141–152.
21. M. Facciotti, V. Boffa, G. Magnacca, L. B. Jørgensen, P. K. Kristensen, A. Farsi, K. König, M. L. Christensen, Y. Yue, Deposition of thin ultrafiltration membranes on commercial SiC microfiltration tubes, Ceram. Int. (2014) 40 3277–3285.
22. V. Boffa, J.E. ten Elshof, D.H.A. Blank, Preparation of templated mesoporous silica membranes on macroporous α-alumina supports via direct coating of thixotropic polymeric sols, Microporous Mesoporous Mater. (2007) 100 173–182.
23. S.Lee, G. Park, G. Amy, S. K. Hong, S.H. Moon, D. H. Lee, J. Cho, Determination of membrane pore size distribution using the fractional rejection of nonionic and charged macromolecules, J. Membr. Sci. 201 (2002) 191–201.
24. K. J. Kim, A. G. Fanen, R. Ben Aim, M. G. Liu, G. Jonsson, I. C. Tessaro, A. P. Broek, D. Bargeman, A comparative study of techniques used for porous membrane characterization: pore characterization, J. Membr. Sci. 81 (1994) 35–46.
25. L.V. Interrante, C.W. Whitmarsh, W. Sherwood, H.-J. Wu, R. Lewis, G. Maciel, High yield polycarbosilane precursors to stoichiometric SiC. Synthesis, pyrolysis and application, Mater. Res. Soc. Symp. Proc. 346 (1994) 593–603.
26. J.P.Olivier, Modeling physical adsorption on porous and non porous solids using density functional theory, J.PorousMater. 2 (1995) 9–17.

27. P. M. Biesheuvel, H. Verweij, Design of ceramic membrane supports: permeability, tensile strength and stress, J. Membr. Sci. 156 (1999) 141–152.
28. H. Qi, S. Niu, X. Jiang, N. Xu, Enhanced performance of a macroporous ceramic support for nanofiltration by using α-Al2O3 with narrow size distribution, Ceram. Int. 39 (2013) 2463–2471.
29. W.X. Deng, X.H. Yu, M. Sahimi, T. T. Tsotsis, Highly permeable porous silicon carbide support tubes for the preparation of nanoporous inorganic membranes, J. Membr. Sci. 451 (2014) 192–204.
30. L. V. Interrante, I. Rushkin and Q. Shen, Linear and Hyperbranched Polycarbosilanes with Si-CH2-Si Bridging Groups: A Synthetic Platform for the Construction of Novel Functional Polymeric Materials, Appl. Organometal. Chem. 12 (1998) 695–705.
31. V. Médout-Marère, et al., Surface heterogeneity of passively oxidized silicon carbide particles: hydrophobic–hydrophilic partition, J.Colloid Interface Sci. 223 (2000) 205–214.
32. Narnedra B. Dahotre, T.S. Sudarshan, Intermetalic and ceramic coatings, CRC Press, 1999.
33. Minghui Qui, Yiqun Fan, Nanping Xu, Preparation of supported zirconia ultrafiltration membranes with the aid of polymeric additives, J. Membr. Sci. 348 (2010) 252–259.
34. J. H. Dymond, H. A. Øye Viscosity of Selected Liquid n-Alkanes J. Phys. Chem. Ref. Data 23 (1994) 41–53.
35. R. Sreeja, B. Swaminathan, A. Painuly, T.V. Sebastian, S. Packirisamy, Allylhydridopolycarbosilane (AHPCS) as matrix resin for C/SiC ceramic matrix composites, Mater. Sci. Eng. B 168 (2010) 204–207.
36. M. Kotani, Y. Katoh, A. Kohyama. M. Narisawa, Fabrication and Oxidation -Resistance Property of Allylhydridopolycarbosilane-Derived SiC-SiC Composites, J. Ceram. Soc. JPN 111 (2003) 300–307.

37. A. R. Maddocks, D. J. Cassidy, A. S. Jones, A. T. Harris, Synthesis of nanoporous silicon carbide via the preceramic polymer route, Mater. Chem. Phys. 113 (2009) 861–867.
38. A.Larbot, S.Alami-Younssi, M.Persin, J.Sarrazin, L.Cot, Preparation of a γ-alumina nanofiltration membrane, J.Membr.Sci. 97 (1994) 167–173.
39. R.J.R. Uhlhorn, M.H.B.J.Huisin't Veld, K.Keizer, A.J. Burggraaf, Synthesis of ceramic membranes, J.Mater.Sci.27 (1992) 527–537.
40. J. Sekulic, A.Magraso, J.E. ten Elshof, D.H.A. Blank, Influence of ZrO2 addition on microstructure and liquid permeability of mesoporous TiO2 membranes, Microporous Mesoporous Mater. 72 (2004) 49–57.
41. T.Tsuru, D.Hironaka, T.Yoshioka, M.Asaeda, Titania membranes for liquid phase separation: effect of surface charge on flux, Sep.Purif.Technol.25 (2001) 307–314.
42. T.Tsuru, H.Takezoe, M.Asaeda, Ion separation by porous silica–zirconia nanofiltration membranes, AIChEJ.44 (1998) 765–768.
43. T.Tsuru, H.Takezoe, S.Wada, S.Izumi, M.Asaeda, Silica–zirconia membranes for nanofiltration, J.Membr.Sci.149(1998)127–135.
44. V. Boffa, J.E. ten Elshof, A.V.Petukhov, D.H.A.Blank, Microporous niobia–silica membrane with very low CO2 permeability, ChemSusChem 1 (2008) 437–443.
45. A.J.Burggraaf, L.Cot, Fundamental sof Inorganic Membrane Science and Technology, Elsevier, Amsterdam (1996) 74.

Table 1: SiC membranes coated on macroporous SiC disks and their quality as observed by SEM analysis.

Membrane	Solvent	α-SiC loading (% w/w)	AHPCS/α-SiC ratio (w/w)	Film quality
M1	n-hexane	3	0.2	discontinuous
M2	n-hexane	5	0.2	**good**
M3	n-hexane	7	0.2	large cracks
M4	n-hexane/ tetradecane (70:30)	3	0.2	loose particles, large pores
M5	n-hexane/ tetradecane (70:30)	5	0.2	many small cracks
M6	n-hexane/ tetradecane (70:30)	7	0.2	many small cracks
M7	n-hexane/ tetradecane (70:30)	3	0.7	no cracks, large pores
M8	n-hexane/ tetradecane (70:30)	3	1.0	no cracks, large pores
M9	n-hexane/ tetradecane (70:30)	3	1.7	many large cracks
M10	n-hexane	5	0.6	**good**
M11	n-hexane	5	0.8	**Good**

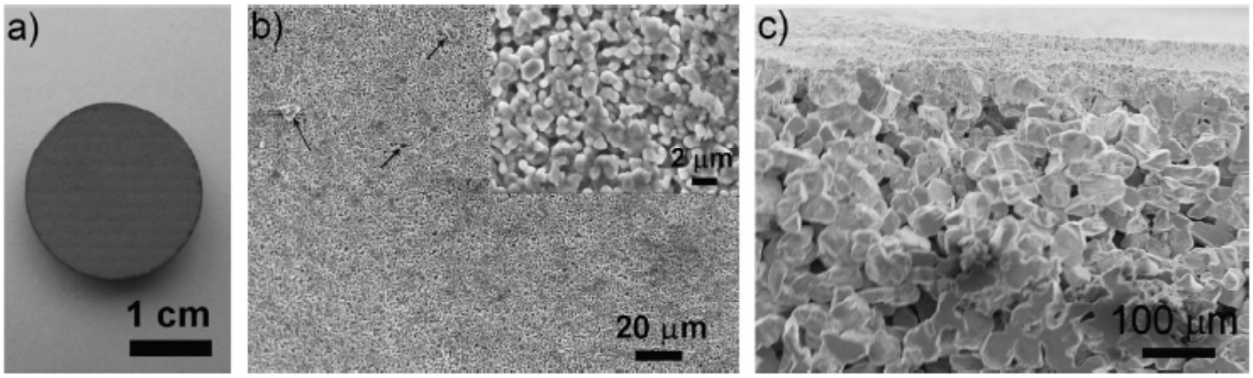

Fig. 1.(a) Macroscopic view and (b) SEM micrograph of the macroporous SiC disk support and (c) SEM micrograph of the cross-section of the SiC support.

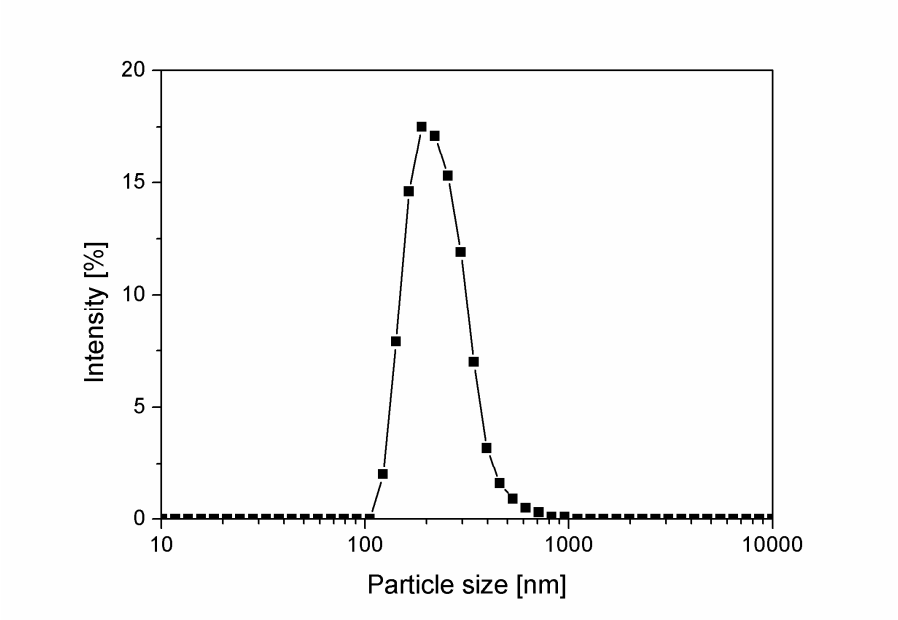

Fig. 2. Particle size distribution of the used α-SiC powder

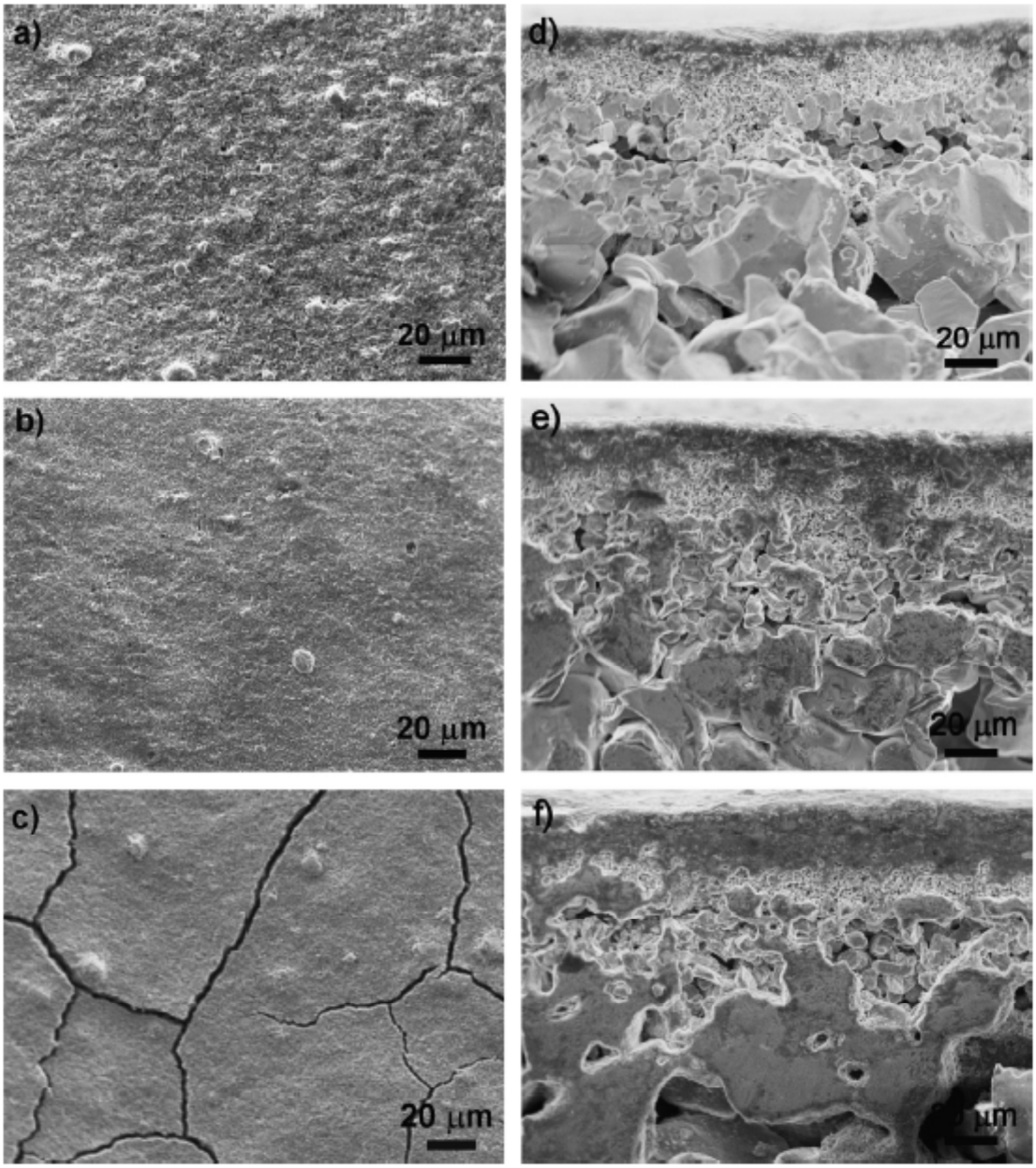

Fig. 3. SEM micrographs of the surfaces and of the cross-sections of heat-treated coatings prepared from n-hexane suspensions with AHPCS/ α-SiC=0.2 and (a,d) 3% α-SiC powder (membrane M1), (b,e) 5% α-SiC powder (membrane M2) and (c,f) 7% α-SiC powder (membrane M3)

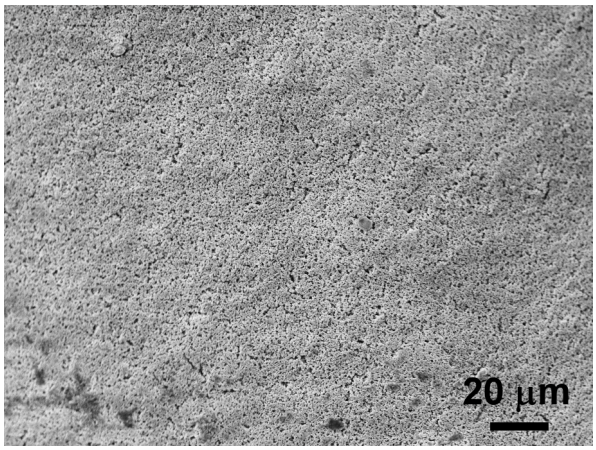

Fig. 4. SEM micrograph of heat-treated coating M4 prepared from suspension with ratio AHPCS/ α-SiC = 0.2 and 3% α-SiC powder in n-hexane/ tetradecane (70:30).

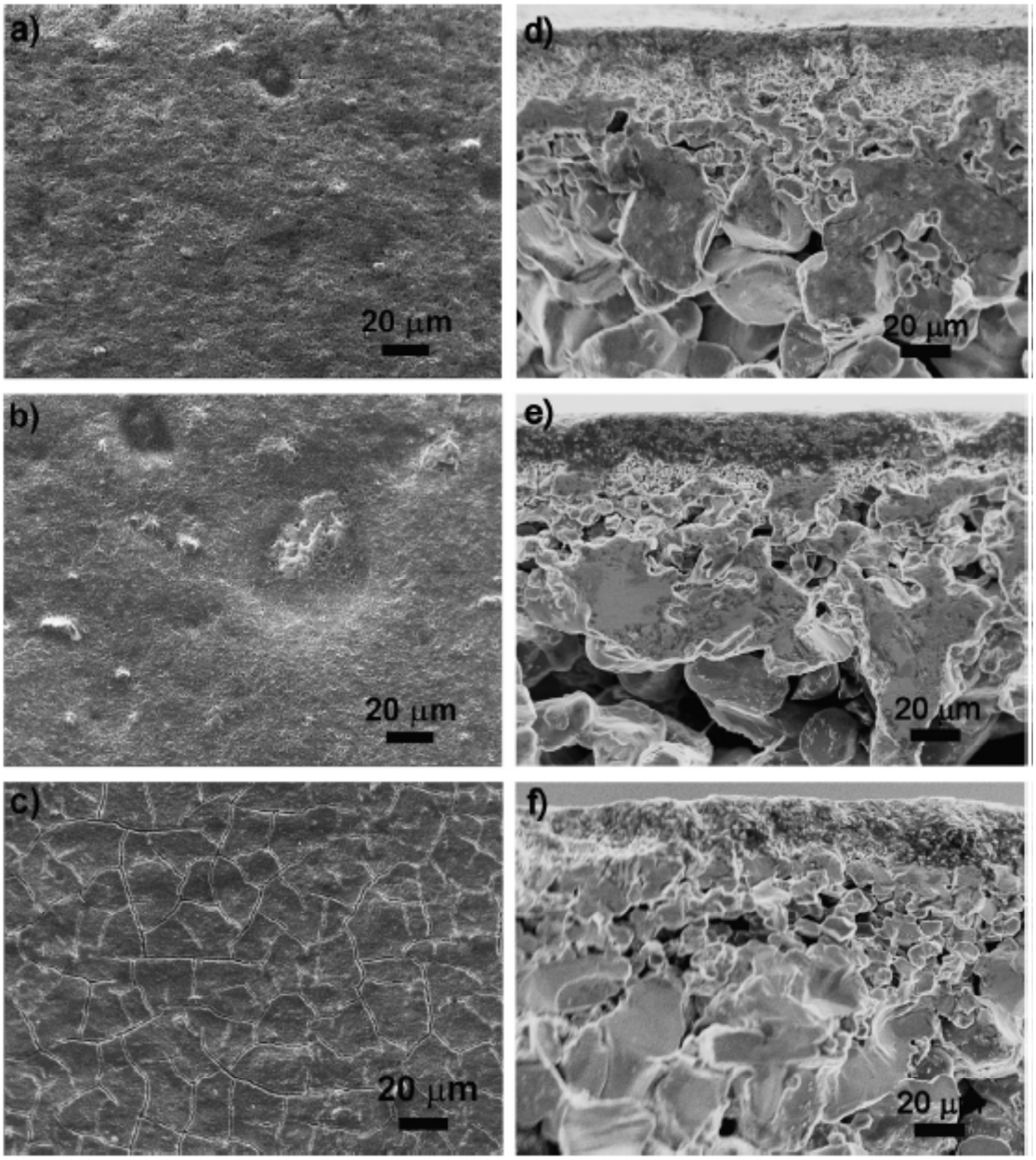

Fig. 5. SEM micrographs of the surfaces and of the cross-sections of heat-treated coatings prepared from suspensions with 3% α-SiC powder in n-hexane/ n-tetradecane (70:30) and ratio (a,d) AHPCS/ α-SiC = 0.7 (membrane M7), (b,e) AHPCS/ α-SiC = 1 (membrane M8) and (c,f) AHPCS/ α-SiC = 1.7 (membrane M9).

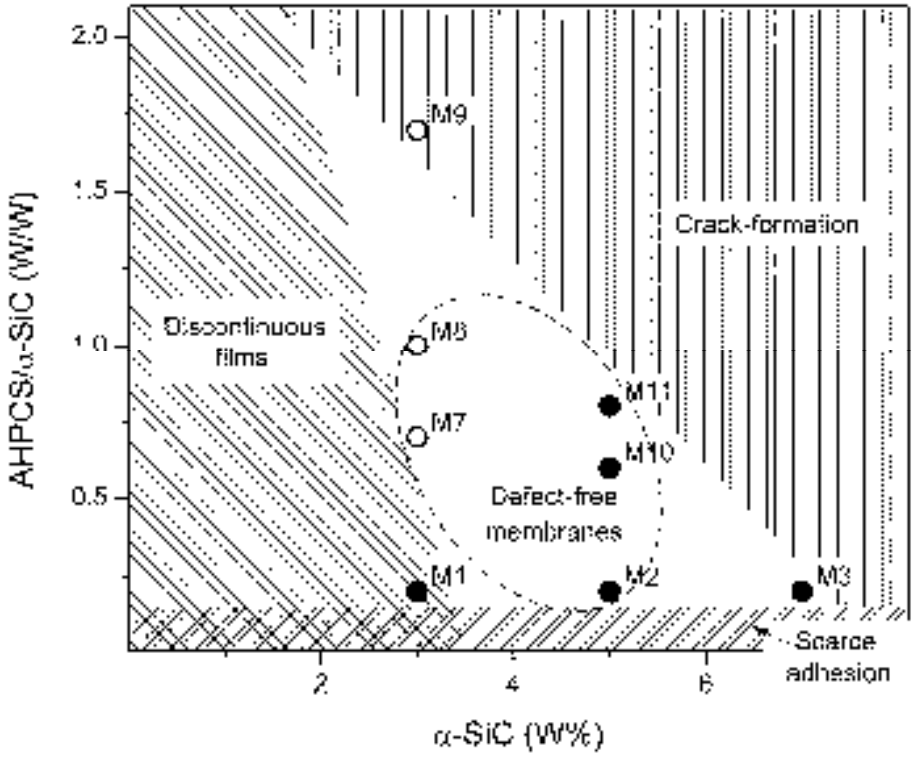

Fig. 6 Schematic presentation of the quality of the obtained membranes as a function of ratio AHPCS/ α-SiC powder and α-SiC powder content. Filled circles denote the membranes prepared from suspensions in n-hexane, empty circles denote the membranes prepared from suspensions in n-hexane/tetradecane (70:30). Area inside of the dashed ellipse border denotes suspension compositions where defect-free membranes were fabricated.

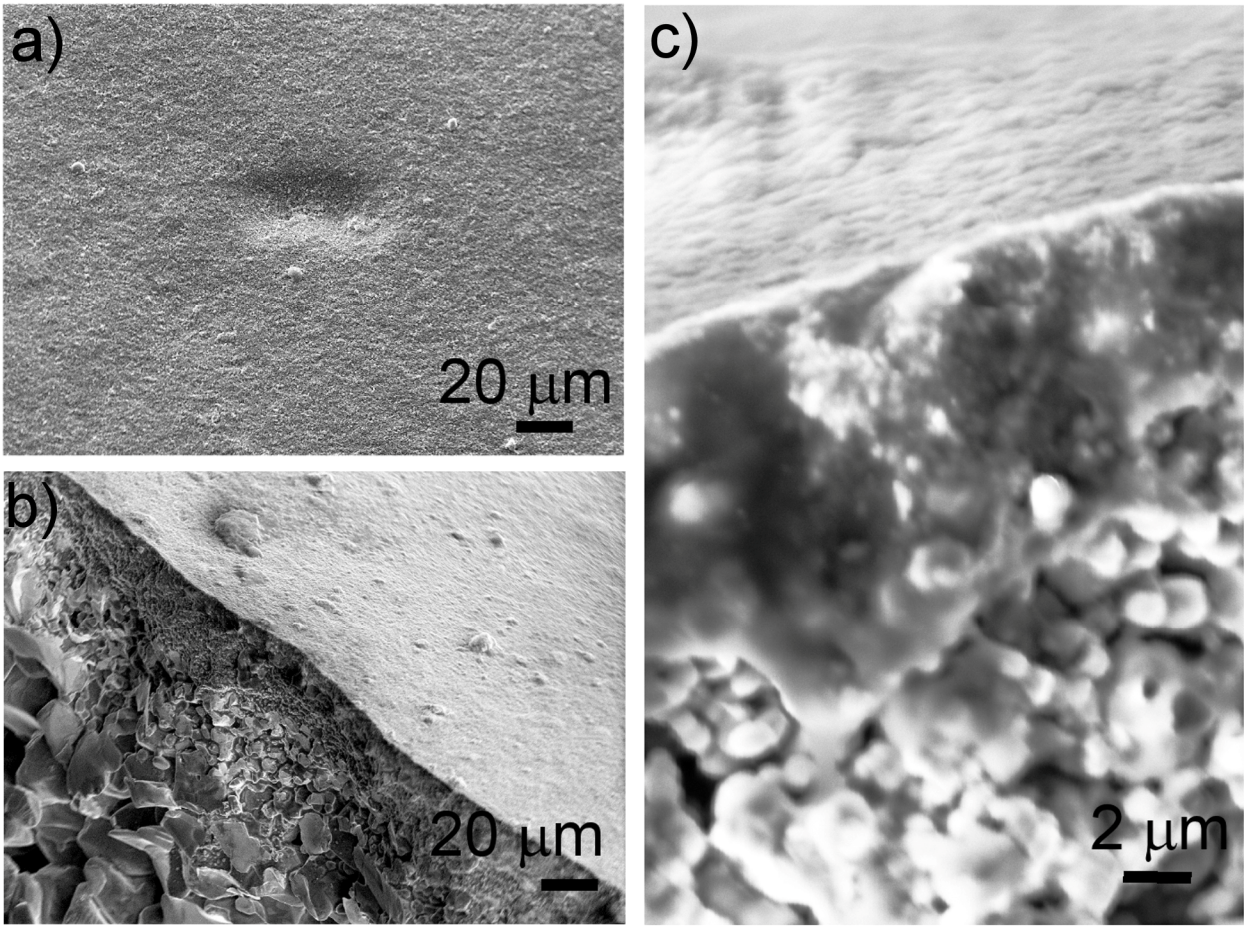

Fig. 7. SEM micrographs of heat-treated coating M10, prepared from a suspension with 5% α-SiC powder in n-hexane, ratio AHPCS/ α-SiC=0.6: (a) surface, (b) cross-section and (c) cross- section at higher magnification.

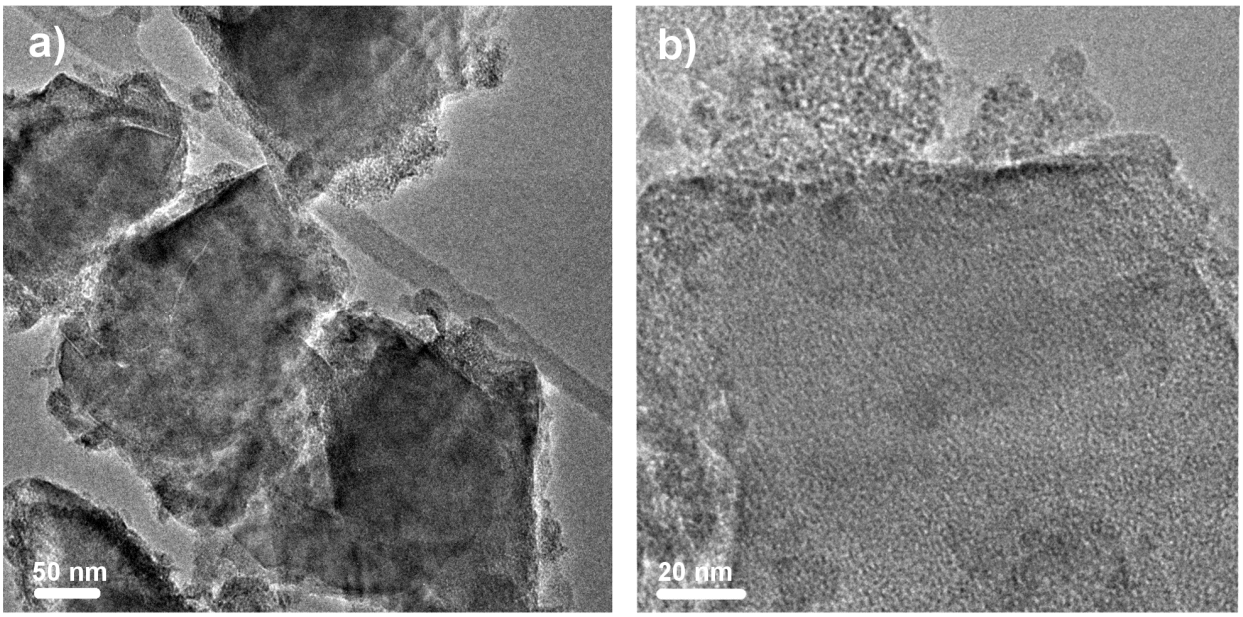

Fig. 8. (a), (b) TEM images of the heat-treated unsupported membrane sample M10 (5% α-SiC powder, ratio AHPCS/ α-SiC = 0.7 in n-hexane) at different magnifications

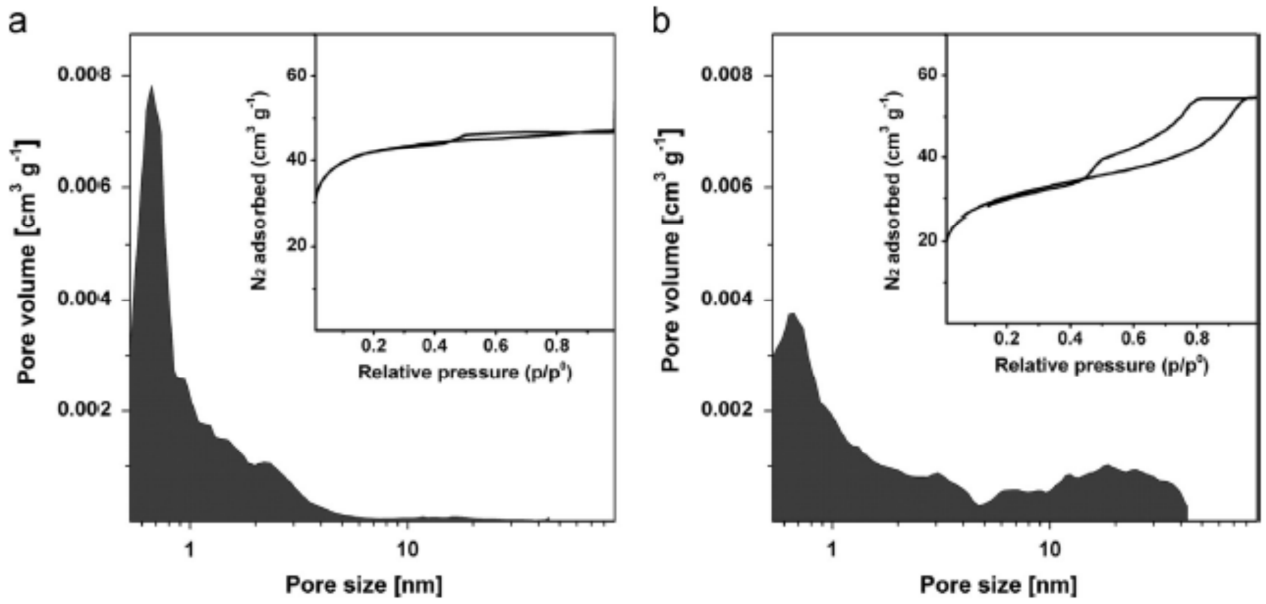

Fig. 9. Pore size distribution of the heat-treated unsupported membranes: (a) M10 (5% α-SiC powder, ratio AHPCS/ α-SiC = 0.6 in n-hexane) and (b) M11 (5% α-SiC powder, ratio AHPCS/ α-SiC = 0.8 in n-hexane). These pore size distributions were calculated from the nitrogen sorption isotherms reported in the corresponding insets by the DFT method.

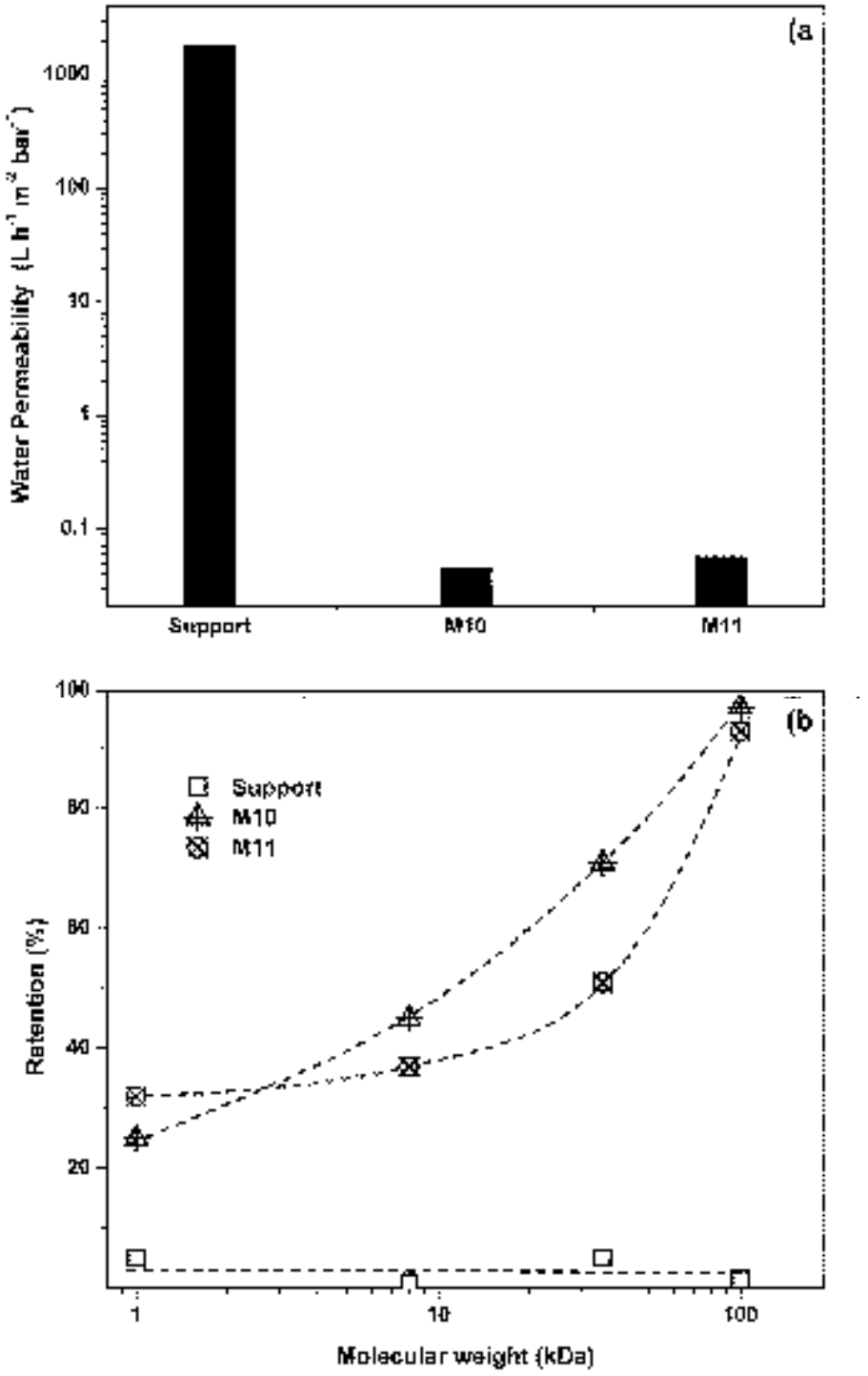

Fig. 10**.** (a) Deionized water permeability and (b) retention towards PEG (1 kDa, 8 kDa, 35 kDa, and 100 kDa) for the as-received support and for the membranes M10 and M11.

-